Secondary instability in drift wave turbulence as a mechanism for zonal flow and avalanche formation

P.H. Diamond, S. Champeaux, M. Malkov, A. Das*, I. Gruzinov, M.N. Rosenbluth, C. Holland, B. Wecht
University of California, San Diego,
La Jolla, California, United States of America

A.I. Smolyakov
University of Saskatchewan,
Saskatoon, Saskatchewan, Canada

F.L. Hinton
General Atomics,
San Diego, California, United States of America

Z. Lin, T.S. Hahm
Princeton Plasma Physics Laboratory, Princeton University,
Princeton, New Jersey, United States of America

Abstract. The article reports on recent developments in the theory of secondary instability in drift–ion temperature gradient turbulence. Specifically, the article explores secondary instability as a mechanism for zonal flow generation, transport barrier dynamics and avalanche formation. These in turn are related to the space–time statistics of the drift wave induced flux, the scaling of transport with collisionality and β, and the spatio-temporal evolution of transport barriers.

1. Introduction

Recently, the role of secondary instability in drift wave turbulence has received considerable attention. This attention has been focused on the role of zonal flows in regulating transport and fluctuations, and on streamers, or radially extended convective cells, as a possible concrete realization of the avalanche concept from self-organized criticality theory in the context of continuum models of plasma dynamics. In this article, several recent results in the theory of secondary instabilities are presented and discussed. In Section 2, the focus is on the theory of zonal flows. First, a physical picture of the mechanism of zonal flow generation is presented. This picture complements earlier theoretical calculations. The solutions of the coupled 'predator–prey' equations for the zonal flow and drift wave spectra are then discussed. In particular, the possibility of bifurcation to a condensate state is demonstrated. The basic theory is also extended to include the effects of zonal flows on the transport cross-phase and to treat the simultaneous evolution of zonal and mean flows. In Section 3, the theory of streamers for ion temperature gradient (ITG) turbulence is presented. The non-linear growth rate for streamers is calculated using modulational instability theory. The processes of streamer saturation via subscale Kelvin–Helmholtz instability and by radial shearing feedback on the underlying turbulence are discussed and compared. The implications of streamer formation for the probability distribution function (pdf) of the transport flux are also identified. In particular, we show that the normalized variance of the flux pdf can easily exceed unity.

2. Zonal flows and transport barriers

Recent computational and theoretical research has demonstrated that zonal flow shear layers are an intrinsic and important constituent of the now classic paradigm of drift–ITG turbulence [1, 2]. By zonal flows, we refer to low frequency, poloidally symmetric potential perturbations with small radial scale

* *Permanent address:* Institute for Plasma Research, Bhat, Gandhinagar 382428, India.

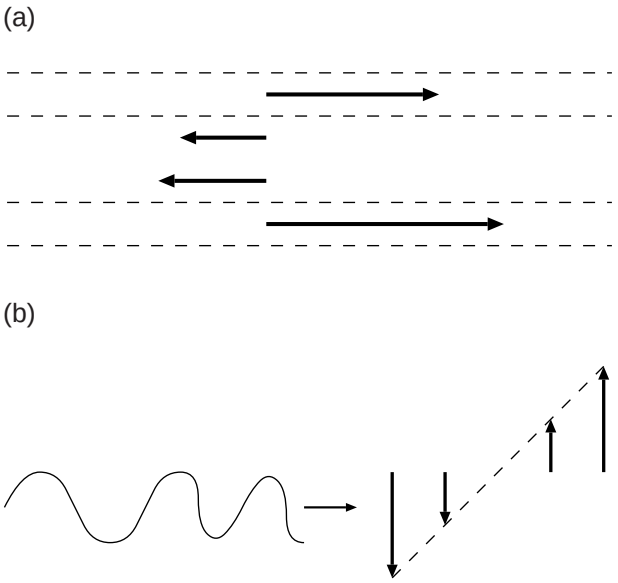

Figure 1. (a) Zonal flows ↔ 'random' $\boldsymbol{E} \times \boldsymbol{B}$ shear. (b) Drift wave in sheared flow field.

(i.e. $k_\theta = 0, k_\| = 0, k_\perp \rho_i$ (finite) [3–5]). In particular, zonal flows are central to the self-regulation mechanisms of drift wave turbulence intensity and transport [6]. In this section, we discuss recent developments in the theory of zonal flows. Special attention is devoted to the basic physics of zonal flow generation, the mechanisms of zonal flow saturation and the effect of zonal flows on transport.

2.1. Basic physics of generation

Zonal flows are shear layers or strongly anisotropic vortices with $k_\theta = 0, k_\| \cong 0, k_\perp \rho$ finite and (nearly) zero frequency, $\Omega \cong 0$. Since $k_\theta = 0, \tilde{V}_r = 0$, so that zonal flows are intrinsically incapable of driving transport, and thus represent a reservoir of benign fluctuation energy. Zonal flows may be thought of as a particular limit ($k_r \gg k_\theta = 0$) of the more general convective cell structure. In contrast to the familiar mean $\boldsymbol{E} \times \boldsymbol{B}_0$ shear flows, with direction determined by profile structure and characterized by a single scale, zonal flows are of indeterminate direction and exhibit a spectrum of scales producing a spatially complex flow profile. Zonal flows are nonlinearly generated by drift waves via modulations of the radial flux of vorticity (i.e. charge separation current [7, 8]) and are damped by ion–ion collisions [9], by non-linear feedback on the underlying drift waves [10] or (possibly) by Kelvin–Helmholtz type instabilities which disrupt them [11].

It is illuminating to present a short, 'back-of-an-envelope' type demonstration of zonal flow instability. Consider a packet of drift waves propagating in an ensemble of quasi-stationary, random zonal flow shear layers, as shown in Fig. 1(a). Take the zonal flows as slowly varying with respect to the drift waves (i.e. $\Omega \ll \omega_{\boldsymbol{k}}$), i.e. quasi-stationary. The spatially complex shearing flow will result in an increase in $\langle k_r^2 \rangle$, the mean square radial wave vector (i.e. consider a random walk of k_r, as described by eikonal theory). In turn the drift wave frequency $\omega_{e^*}/(1 + k_\perp^2 \rho_s^2)$ must then decrease. Since $\Omega \ll \omega_{\boldsymbol{k}}$, the drift wave action density $N(\boldsymbol{k}) = \varepsilon(\boldsymbol{k})/\omega_{\boldsymbol{k}}$ is conserved, so that drift wave energy must also decrease. As the total energy of the system of waves and flows is also conserved (i.e. $\varepsilon_{wave} + \varepsilon_{flow} = \text{const}$), it thus follows that the zonal flow energy must, in turn, increase. Hence, the initial perturbation is reinforced, suggestive of instability. Note that the simplicity and clarity of this argument support the assertion that zonal flow generation is a robust and ubiquitous phenomenon.

A slightly larger envelope is required for a 'physical argument' which is also quantitatively predictive. Consider a drift wave packet propagating in a sheared flow field, as shown in Fig. 1(b). Take $\omega_{\boldsymbol{k}} > |V_E'|$ and $|\boldsymbol{k}| > |V_E'/V_E|$, so that wave action density is conserved (i.e. $N(k) = N_0$, a constant). Thus, wave energy density evolves according to:

$$\begin{aligned}\frac{d}{dt}\varepsilon(\boldsymbol{k}) &= N_0 \frac{d\omega_{\boldsymbol{k}}}{dt} \\ &= N_0 \left(\frac{\partial \omega_{\boldsymbol{k}}}{\partial t} + \boldsymbol{V}_g \cdot \frac{\partial \omega_{\boldsymbol{k}}}{\partial \boldsymbol{x}} + \frac{\partial \omega_{\boldsymbol{k}}}{\partial \boldsymbol{k}} \cdot \frac{d\boldsymbol{k}}{dt} \right) \\ &\cong \left(\frac{2 k_r k_\theta \rho_s^2}{1 + k_\perp^2 \rho_s^2} \right) V_E' \varepsilon(\boldsymbol{k}). \end{aligned} \tag{1}$$

Here we have assumed stationary, isotropic turbulence and have used the eikonal equation $dk_r/dt = -\partial(k_\theta V_E)/\partial x$. Equation (1) just states that the drift wave packet loses or gains energy via work on the mean flow via wave induced Reynolds stress. (Indeed, $k_r k_\theta \varepsilon(\boldsymbol{k}) \sim \langle \tilde{V}_r \tilde{V}_\theta \rangle$!) Note as well that the factor $k_r k_\theta \varepsilon(\boldsymbol{k}) V_E'$ is rather obviously suggestive of the role of triad interactions in controlling fluctuation–flow energy exchange. For zonal flows, the shear is random and broadband, so that $V_E' \to \tilde{V}_E$, $N \to \langle N \rangle + \tilde{N}$ and $N_0 V_E' \to \langle \tilde{N} \tilde{V}_E' \rangle$. Hence, Eq. (1) may be rewritten as:

$$\frac{d}{dt}\varepsilon(\boldsymbol{k}) = -V_{g,r} k_\theta \langle \tilde{V}_E' \tilde{N} \rangle. \tag{2}$$

To complete the argument, the correlator $\langle \tilde{V}'_E \tilde{N} \rangle$ must be calculated. To this end, we use the wave kinetic equation (WKE)

$$\frac{\partial N}{\partial t} + (\boldsymbol{V}_g + \boldsymbol{V}) \cdot \boldsymbol{\nabla} N - \frac{\partial}{\partial \boldsymbol{x}}(\omega + k_\theta V_E) \cdot \frac{\partial N}{\partial \boldsymbol{k}} = \gamma_{\boldsymbol{k}} N - \Delta\omega_{\boldsymbol{k}} N^2/N_0 \quad (3)$$

and the methodology of quasi-linear theory to obtain:

$$k_\theta \langle \tilde{V}'_E \tilde{N} \rangle = D_K \frac{\partial \langle N \rangle}{\partial k_r} \quad (4a)$$

$$D_K = k_\theta^2 \sum_q q^2 |\tilde{V}'_{Eq}|^2 R(\boldsymbol{k}, q) \quad (4b)$$

$$R(\boldsymbol{k}, q) = \gamma_{\boldsymbol{k}} / ((q V_{g,r})^2 + \gamma_{\boldsymbol{k}}^2). \quad (4c)$$

The term $\Delta\omega_{\boldsymbol{k}} N^2/N_0$ represents drift wave non-linear damping via self-interaction of drift waves (i.e. cascade by local interaction).

Here q is the radial wavenumber of the zonal flow, and equilibrium balance in the absence of flow has been used to relate $\Delta\omega_{\boldsymbol{k}}$ to $\gamma_{\boldsymbol{k}}$. The wave energy then evolves according to:

$$\frac{d\varepsilon(\boldsymbol{k})}{dt} = \frac{2\rho_s^2 D_K k_r}{(1 + k_\perp^2 \rho_s^2)^2} \frac{\partial \langle N \rangle}{\partial k_r}. \quad (5)$$

As the total energy of the stationary wave–flow system is conserved,

$$d/dt \left(\sum_{\boldsymbol{k}} \varepsilon(\boldsymbol{k}) + \sum_q |\tilde{V}_q|^2 \right) = 0.$$

Thus, the zonal flow generation rate is determined to be:

$$\gamma_q = -2q^2 c_s^2 \sum_{\boldsymbol{k}} \frac{k_\theta^2 \rho_s^2}{(1 + k_\perp^2 \rho_s^2)^2} R(\boldsymbol{k}, \boldsymbol{q}) k_r \frac{\partial}{\partial k_r} \langle \eta \rangle \quad (6a)$$

$$\langle \eta \rangle = \left(1 + k_\perp^2 \rho_s^2\right) \langle \varepsilon \rangle. \quad (6b)$$

Here $\langle \eta \rangle$ is the mean potential enstrophy density of the drift wave turbulence.

The result given above in Eq. (6a), obtained by transparent physical reasoning, is identical to that derived previously by formal modulational stability arguments [7]. Note that $\partial \langle \eta \rangle / \partial k_r < 0$ (a condition which is virtually always satisfied in drift wave turbulence) is required for zonal flow growth. In addition, the argument above reveals that drift wave ray chaos provides the key element of irreversibility, which is crucial to the wave–flow energy transfer dynamics. Here ray chaos requires overlap of the $\Omega/q = V_{g,r}$ resonances in D_k, a condition easily satisfied for finite lifetime drift wave eddys and (nearly) zero frequency zonal flows (i.e. $\Delta\omega_{\boldsymbol{k}} \gg \Omega$). Under these conditions a positive Lyapunov exponent is present and neighbouring drift wave rays diverge exponentially in time. Ray chaos in turn ensures that zonal flow shearing and wave refraction are random, thus validating the use of the stochastic methodology employed here. In the case where rays are not chaotic, envelope perturbation formalism, methods from the theory of trapping or parametric instability theory must be used to calculate zonal flow generation.

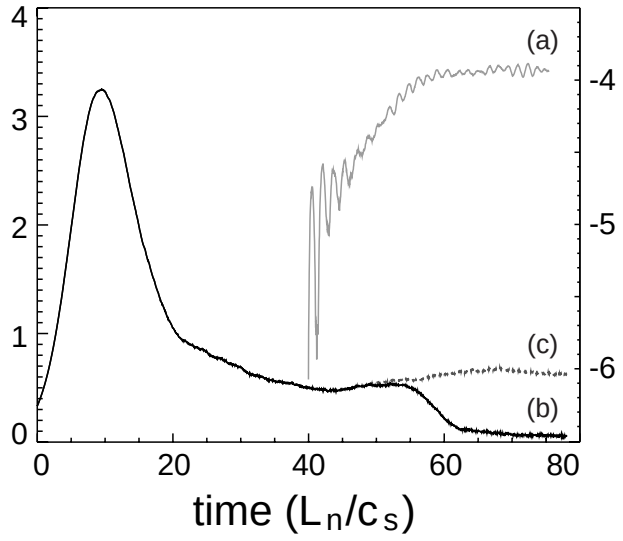

Figure 2. Growth of the zonal flow U_E (a) in a background of fully developed ITG turbulence. Note that χ_i decreases as U_E grows (b), but persists if the zonal flow is absent (c).

Recent gyrokinetic simulations have demonstrated that modulational instability growth of zonal flow perturbations in fully developed drift–ITG turbulence can occur. Figure 2 shows that the evolution of a (seed) zonal flow perturbation initialized in a bath of quasi-stationary ITG turbulence which had already saturated by other processes. The seed perturbation clearly grows exponentially and its growth induces a further decrease in the ion thermal diffusivity, as measured by the simulation. Quantitative comparisons of simulation results with the theory are in progress. Nevertheless, this evidence for the viability of the modulational instability of zonal flows in turbulence, as well as their role in regulating transport, is quite compelling.

The basic theory of zonal flow generation outlined above has been extended to include ITG mode drive (in both coherent [12] and random phase analyses [13]), and to treat the narrow band regime [14] and

the purely weak turbulence regime near the instability threshold. More theoretically oriented investigations have elucidated the nature and dynamics of the quanta density [15] and the behaviour of wave packets when trapped or strongly modulated by zonal flows [16, 17]. Other extensions have treated coupling to electromagnetic fluctuations in the regime of finite β [18, 19], and the generation of zonal fields [20] (magnetic perturbations with a structure analogous to that of zonal flows), a phenomenon with many similarities to the small scale dynamo. Finally, the modulational instability theory has been used to calculate the cross bi-spectrum of large scale potential with small scale perturbations, and to guide experimental investigations of non-linear interactions at the $L \rightarrow H$ transition, where zonal flow growth can be expected [21, 22]. Readers interested in any of the aforementioned topics are referred to the literature cited here.

2.2. Mechanisms for zonal flow saturation

In this section, we discuss the critical question of how the drift wave–zonal flow (DW–ZF) system saturates. There are basically two possible routes to saturation, namely via self-regulation by feedback of the ZFs on the DW spectrum, and via destruction of the ZFs by Kelvin–Helmholtz type instability. Here we present recent results on self-regulation. We solve the coupled equations for the DW and ZF spectra for arbitrary finite flow collisionality. In particular, we determine the crossover between $\langle N \rangle \sim \gamma_d$ scaling (noted previously [23]) and $\langle N \rangle$ independent of γ_d (at large γ_d) scaling, reminiscent of mixing length estimates. We also discuss the condensate type solutions which appear. The latter may be related to the formation of jets or streamers.

As we mentioned, ZFs in toroidal devices are linearly damped only by collisions and may thus develop quite complicated radial structures that can hardly be captured by models with only a small number of modes. This necessitates a theory capable of describing DWs and ZFs as coupled elements of the corpus of self-organized turbulence without lumping their spectra into a few spectral components. Our predator–prey approach has an advantage over the low dimensional models since it is based on a spectral description of the turbulence. We have studied the stationary spectra of coupled DW–ZF turbulence from the perspective of this model. The focus is on the scaling of the turbulence and transport levels with the ZF collisional damping, γ_d.

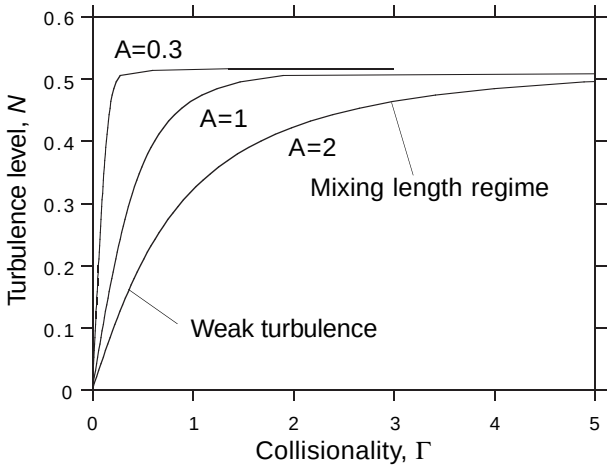

Figure 3. Level of the DW turbulence N (normalized to twice the mixing length level) for the regular spectrum as a function of the collisional damping of the ZFs normalized to the growth rate γ, $\Gamma = \gamma_d/\gamma$. For stronger self-non-linearity of the DWs (smaller A), the transition to the mixing length regime is naturally faster.

The analysis entails a natural division of the DW spectrum into two physically distinct regions. One region is that of excitation by the ITG instability and the other is where the DWs are linearly and nonlinearly damped. The flux of the DW quanta from the former to the latter is determined by the level of the ZF turbulence, which, as we mentioned, is in turn powered by the DWs themselves. The transfer occurs via random shearing of drift waves by ZFs. Depending on the relation between the timescales of ZF damping and DW generation γ_d/γ, two distinct regimes occur. If this ratio is small, the DWs are very efficiently sheared by ZFs, so that their amplitude scales linearly with γ_d. If γ_d/γ is large, the DWs saturate via their own non-linearity and the turbulence level will be independent of γ_d (Fig. 3). Of course, determining the value of γ_d/γ at the crossover is especially critical to predictions of transport scaling.

It turns out, however, that multiple saturated states are possible. Starting from a critical ZF damping rate $\gamma_d = \gamma_c$, two new solutions with considerably higher intensity DW level branch off from the expected one. Of the three solutions in total, the intermediate one is (presumably) unstable (Fig. 4). The solution with smaller turbulence intensity (with saturation via γ_d) is characterized by strong shearing of DWs. The solution with higher intensity, based on its spectral properties (condensate in k_r), consists of radially elongated features in the DW

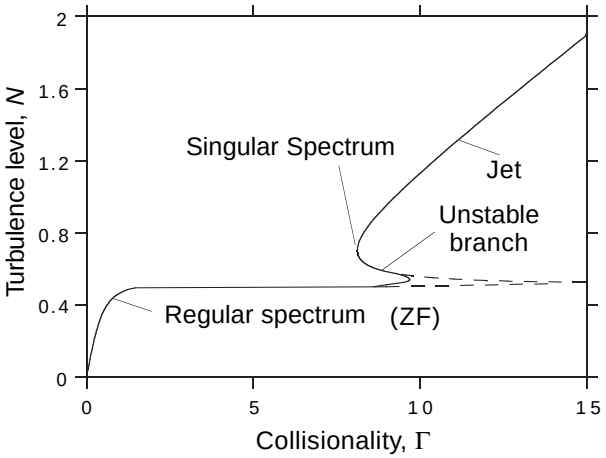

Figure 4. The same as in Fig. 3 but for both the regular and the singular (condensate) solutions. The condensate spectrum (upper branch) is more easily destroyed by the ZFs if this spectrum is radially more extended (smaller value of the cut-off parameter k_{min}). The left cusp on the bifurcation diagram shifts to the right with decreasing k_{min} (not shown).

turbulence which can be tentatively identified with jets or streamers. Cyclic bifurcation transitions between these two states, reminiscent of the bursting states observed in simulations [23], are possible.

By studying these solutions we have addressed the following issues: (i) the saturation mechanism of the DW turbulence far from the threshold of linear stability, (ii) determining the transition region from linear scaling with γ_d to saturation independent of γ_d, (iii) determining the forms of the stationary DW $\langle N(k_r)\rangle$ and ZF spectra $|\phi_q|^2$, (iv) the stability of stationary solutions.

The principal results of this study are the following:

(1) In the limit of weak ZF damping, $\gamma_d\Delta\omega/\gamma^2 \ll 1$, the DW turbulence level, and thus transport, scale with collision rate as $\langle N\rangle \propto \gamma_d/\gamma$, in agreement with previous results.
(2) In the opposite limit of strong collisional damping of ZFs, $\gamma_d\Delta\omega/\gamma^2 \ll 1$, DWs saturate at a level independent of collisionality, which is roughly consistent with mixing length predictions. Crossover occurs at $\gamma_d\Delta\omega/\gamma^2 \approx 1$. This behaviour is robust, the solution is linearly stable and no turbulent viscosity need be assumed for saturation.
(3) Starting from a critical γ_d, two new solutions branch off. They manifest a ZF induced inverse energy transfer within the DW component of the turbulence. They have a significantly higher level of turbulence and transport. Their spectral behaviour as $k_r \to 0$ is that of a condensate type (i.e. a cut-off $k_r = k_{min}$ is required since $\langle N\rangle \propto 1/k_r^2$), and the corresponding spatial structures are radially elongated, i.e. jets or streamers.

Even though the stability analysis predicts multiple states, we were able to identify the lowermost branch of the solution (which tracks γ_d and ultimately saturates) with a clearly generic response of the self-regulated DW–ZF system to the collisional self-damping γ_d. The change of the turbulence regime occurs when the parameter $\gamma_d\Delta\omega/\gamma^2$ (roughly) becomes larger than unity, manifesting a situation in which the ZF collisional suppression and the DW non-linear damping dominate production. Loosely speaking, this corresponds to a regime of strong damping of ZFs. The underlying saturated DW spectrum is regular in k and stable. For a simple model of linear instability and non-linear damping of the DWs, we were able to calculate $\langle N\rangle$ in a closed form that has the aforementioned regimes as simple limiting cases.

Besides this solution regular in k_r, there are two singular solutions with higher $\langle N\rangle$ that branch off at sufficiently strong ZF damping γ_d. The 'condensate' or 'jet' spectra (since they are still quite extended, i.e. low k_r) may very well be relevant to the streamer and transport event formation observed in simulations, because of their radially elongated spatial structure. It is interesting to note that the conditions under which the jet spectra should form (strong damping of ZFs) are thus also intrinsically favourable to the development of streamers. Conversely, when the ZFs are not strongly suppressed, they should restrict streamer formation. We summarize our (tentative) results on the condensate and jets below:

(a) Jets require strong suppression of ZFs, i.e. well developed streamers and ZFs do not coexist.
(b) The γ_d threshold for jets is very sensitive to $k_{min} \sim 1/l_{streamer}$. Note that this suggests that flux tube and full geometry simulations may arrive at different results. Formation of systemwide jets would require complete suppression of ZFs.
(c) The onset of the jet regime should not necessarily be accompanied by a significant shift of the DW spectrum to smaller k_r. Owing to the increased role of the DW non-linearity, the spectral broadening is a competing regulatory process in this regime.

(d) On the basis of bifurcation diagrams derived from our results (Fig. 4), bursting may appear as a hysteresis loop phenomenon, i.e. transitions between the ZF dominated (i.e. regular) and condensate solutions can occur.

Note that in addition to determining scalings and spectra as a function of γ_d, this investigation has revealed the existence of a possible condensate spectrum suggestive of streamer or jet formation. Moreover, our results indicate the possibility of cyclic bifurcations between states dominated by ZFs (with small DW eddys) and those dominated by streamers. Phenomena similar to the proposed cyclic bifurcations between these two states have recently been observed in simulations.

2.3. Zonal flow effects on transport

Virtually all of the existing work on zonal flows has focused on the issues of zonal flow generation and damping, as well as their impact on fluctuation levels. However, zonal flows clearly will have a related, but technically distinct, effect on transport. Here we consider two questions, namely that of the impact of zonal flows on the transport cross-phase, and that of how zonal flow effects might be included in a simple model of transport barrier dynamics.

It is well known that mean electric field shear alters the correlation time which is used in constructing the turbulent transport coefficient. This alteration occurs via enhanced Doppler dispersion and enhanced decorrelation [24]. For the case of zonal flows, however, the methodology of Ref. [24] is not applicable, since the zonal flow field is stochastic and spatially complex. Thus, one must treat $R(\omega, \boldsymbol{k})$, the time history of a particle's response to a transport driving perturbation, by averaging over an ensemble of shears, as well as fluctuation driven radial excursions. Specifically, instead of

$$R(\omega, k) = \int_0^\infty d\tau \langle \exp\left[i(\bar{\omega} - k_\theta \tilde{v}'_E \delta x)\tau\right]\rangle_{\delta x} \tag{7a}$$

one must consider

$$R(\omega, \boldsymbol{k}) = \int_0^\infty d\tau \langle \exp[i(\bar{\omega} - k_\theta \tilde{v}'_E \delta x)\tau]\rangle_{\delta x, \tilde{v}'_E}. \tag{7b}$$

Here v'_E is the mean shear, $\bar{\omega}$ is the locally Doppler shifted flow, $\tilde{v}'_E$ is the zonal shear and δx is the particle excursion. Treating the product $\tilde{v}'_E \delta x$ as a random variable and using the standard methodology of cumulant expansions then gives

$$R(\omega, \boldsymbol{k}) = \int_0^\infty \exp[i\bar{\omega}\tau - k_\theta^2 \tau^2 \langle (\tilde{v}'_E \delta x)^2\rangle] d\tau. \tag{8}$$

Assuming $\tilde{v}'_E$ and δx to be statistically independent (NB: This is a step which should be investigated further!) gives

$$\begin{aligned}\langle (\tilde{v}'_E \delta x)^2\rangle \tau^2 &\cong \langle (\tilde{v}'_E)^2\rangle \langle \delta x^2\rangle \tau^2 \\ &= \langle (\tilde{v}'_E)^2\rangle D\tau^3. \end{aligned} \tag{9}$$

Thus

$$R(\omega, \boldsymbol{k}) = \int_0^\infty \exp[i\bar{\omega}\tau - k_\theta^2 D\langle (\tilde{v}'_E)^2\rangle \tau^3] \tag{10a}$$

so that the effective decorrelation rate and resonance broadening is

$$1/\tau_{ceff} = \left(k_\theta^2 \langle (\tilde{v}'_E)^2\rangle D\right)^{1/3} \tag{10b}$$

$$\langle \tilde{v}'^2_E\rangle = \sum_{\boldsymbol{q}} q_x^2 |\tilde{v}_{E,q}|^2. \tag{10c}$$

This effective decorrelation rate for radial transport in random straining fields is easily testable by gyrokinetic simulation. Note that, not surprisingly, the result corresponds to that of Ref. [23], with $(\langle v_E\rangle')^2$ replaced by $\langle (\tilde{v}'_E)^2\rangle$. It should be said, however, that other than barrier regimes, where turbulence and thus zonal flow drive are presumably quenched, $\langle (\tilde{v}'_E)^2\rangle > (\langle v_E\rangle')^2$, so that random shear decorrelation (due to zonal flows) is likely to be dynamically more significant than mean shear decorrelation. Hence, transport evolution models incorporating cross-phase evolution effects should be extended to include the zonal flow induced cross-phase as well.

Another related issue is that of how zonal flows influence the evolution of profiles in general and transport barrier formation in particular. In the past 1-D profile dynamics has been calculated using simple $K-\varepsilon$ type models [25] which evolve the local (at a given r) fluctuation intensity, mean flows and profiles, using transport and momentum balance equations, the radial force balance equation for the mean $\boldsymbol{E}\times\boldsymbol{B}$ velocity $\langle v_E\rangle$ and a model fluctuation intensity evolution equation. To incorporate the effects of zonal flows, which are clearly a crucial player in the physics of the underlying (L mode) transport, several extensions of the theory are required. Specifically,

(1) The fluctuation intensity spectrum $\langle N(k_r)\rangle$ must be evolved using the quasi-linear WKE.

(2) The zonal flow intensity spectrum must be evolved.
(3) The mean profile and electric field shear should be evolved, including zonal flow effects on the cross-phase.

Thus, a slightly less simplified version of the simple model of Ref. [25] (for density evolution only, for simplicity) would be:

$$\frac{\partial\langle N\rangle}{\partial t} - k_\theta\langle v^E\rangle'\frac{\partial\langle N\rangle}{\partial k_r} - \frac{\partial}{\partial k_r}D_k\frac{\partial\langle N\rangle}{\partial k_r} = \gamma_{\boldsymbol{k}}(n')\langle N\rangle - \Delta\omega_{\boldsymbol{k}}\langle N\rangle^2/N_0 \tag{11a}$$

$$\left(\frac{\partial}{\partial t} + \gamma_d\right)|\phi_q|^2 = -q^2c_s^2\sum_{\boldsymbol{k}}\frac{k_\theta^2\rho_\theta^2}{(1+k_\perp^2\rho_s^2)}\frac{\partial\langle N\rangle}{\partial k_r}R(\boldsymbol{k},\boldsymbol{q})|\phi_q|^2 + \text{noise} \tag{11b}$$

$$\frac{\partial n}{\partial t} = S(r) + \frac{\partial}{\partial r}(D_{Neo} + D[\langle N\rangle])\frac{\partial n}{\partial r} \tag{11c}$$

$$\langle v_E\rangle' = -\frac{1}{eB_0}\left(\frac{1}{n}\frac{dP_i}{dr}\right). \tag{11d}$$

Here D_k is given earlier, $\gamma(n')$ denotes the need to incorporate mean gradient evolution in the growth rate, $D[\langle N\rangle]$ is the transport coefficient to be computed using $\langle N(k_r)\rangle$ and $R(\omega,\boldsymbol{k})$ as given by Eq. (10a), $|\phi_q|^2$ is the radial spectrum evolution and Eq. (11d) is the radial spectrum force balance equation. Additional, similar equations can be added for $\langle T_i\rangle$, $\langle v_\phi\rangle$ and $\langle v_\theta\rangle$. Note that detailed calculations indicate that $\langle v_E\rangle'$ effects do not significantly modify D_k, the zonal flow induced k space diffusivity.

3. Towards a dynamical theory of avalanches

3.1. Introduction

Traditionally, the problem of predicting the turbulent transport in magnetically confined plasmas has been approached from the perspective of mean field theory, namely by proceeding from the assumption that the transport dynamics is well described by average fluxes and local transport coefficients, such as effective diffusivities. This mean field/local transport perspective is the underpinning of the often used 'mixing length rule', $D = \gamma_L/k_r^2$, which tacitly presumes that a single time scale (γ_L^{-1}) and a single space scale (k_r^{-1}) are sufficient to characterize the turbulent transport process. Indeed, such mixing length 'guesstimates' are crucial to all of the 'predictive transport models' (such as the IFS–PPPL model and various imitations thereof) currently used in the magnetic fusion energy community. However, the arrival of ideas originating from self-organized criticality (SOC) theory [26, 27], which proposes that a scale invariant spectrum of 'transport events' or 'avalanches' is at work in the dynamics of transport, has stimulated a series of experimental and computational investigations which have cast considerable doubt upon the traditional mean field picture. In particular, experimental studies have yielded:

(a) The direct observation and visualization of avalanche type structures on the DIII-D tokamak [28].
(b) The observation that the pdf of the transport flux is quasi-Gaussian on the scale of the turbulence correlation length but strongly non-Gaussian on larger scales, which is indicative of the formation of structures akin to avalanches [29].
(c) The observation that the pdf of the transport flux exhibits finite size scaling, i.e. $P(\Gamma) = (1/L)P(\Gamma/L)$, where Γ is flux and L is a scaling parameter related to the turbulence intensity [30]. This scaling is observed over a broad range of transport event (i.e. avalanche) sizes.
(d) A wealth of indirect evidence for avalanche and SOC type phenomena, such as the observation of multifractality in turbulence [31] and measurements of $1/f$ type spectra of the turbulent flux [32].

Also, both continuum and particle simulations of familiar turbulence models (ITG, resistive ballooning, etc.) have noted that:

(1) Extended, mesoscale transport events or avalanches are observable and prominent near marginality [33–35].
(2) Anisotropic (radially extended but poloidally narrow) eddys, called streamers, are observable and are clearly related to transport events or bursts. The observed streamers are nonlinear structures, involving many n numbers and evolving on timescales distinct from that of the linear growth rate [36, 37].
(3) Contribution to the total flux from large events diverges, so that scale independent transport

(i.e. 'Bohm') is manifested in models which naively appear to be linked to small scales ('gyro-Bohm') [35].

It should be noted that great care must be taken in designing computational experiments to study avalanches. In particular, experience indicates that global simulations are more accurate than 'flux tube codes', which impose unphysical constraints on mesoscale structures [2, 38]. Similarly, a fixed flux boundary condition, rather than the traditional, convenient but unphysical assumption of a frozen gradient, reveals considerably richer avalanche dynamics [33–35]. All told, there is clearly sufficient, compelling evidence to warrant a detailed study of the dynamics of avalanches.

Theoretical paradigms for avalanche phenomena have been limited to approximate solutions of discrete (cellular automata) models of sandpiles [39] and to the analysis of highly simplified, reduced 1-D models [40, 41]. In particular, there is definitely a gap between these rather idealized systems and even comparatively simple continuum models of turbulence in confined plasmas. In this section, we present a theory of avalanche dynamics for a simple, two field model of ITG turbulence. We conceive of the avalanche as a radially extended, poloidally asymmetric convective cell, called a streamer, and tackle the calculation of its evolution with the methods of modulational stability theory. This approach is thus an extension of the theory of convective cell formation developed by Sagdeev et al. [42], Okuda and Dawson [43], and Kodama and Taniuti [44] in the 1970s. However, we extend the aforementioned paradigm by considering:

(a) The role of magnetic curvature, the pressure advection non-linearity and proximity to marginal stability in streamer formation.
(b) The self-regulation of streamer cells by the feedback of their poloidally sheared radial flows upon the underlying ITG instabilities which support them, and by Kelvin–Helmholtz type instability, which causes their break-up.
(c) The effect of streamers on the statistics of the flux. In particular, we demonstrate the proportionality of the variance of the flux to the streamer intensity level. This simple argument thus bridges the gap between the statistical theory of self-organized criticality and the continuum dynamics of familiar plasma turbulence models.

To avoid possible confusion, we emphasize here that our nomenclature 'streamer' denotes a nonlinear structure, not the linear ballooning mode cells seen in simulations during the linear growth phase. The relevance of the latter to the time asymptotic turbulence dynamics is dubious.

3.2. Theory of streamer dynamics

We consider the simplest possible model of curvature driven ITG turbulence. The basic equations are [45]

$$(\partial_t - \boldsymbol{\nabla}\phi \times \boldsymbol{z}\cdot\nabla)(1-\nabla^2)\phi + v_{*_n}\partial_y\phi + v_B\partial_y p + \nu_0\nabla^2\nabla^2\phi = 0 \quad (12a)$$

$$(\partial_t - \boldsymbol{\nabla}\phi \times \boldsymbol{z}\cdot\nabla)p - \chi_0\nabla^2 p = v_{*_p}\partial_y\phi. \quad (12b)$$

Here the equations are de-dimensionalized by $k\rho \to k, \Omega_i t \to t, e\phi/T \to \phi, p/p_0 \to p$, so that $v_{*_p} = \rho/L_p$, $v_{*_n} = \rho/L_n$ and $v_B = \rho/L_B$. Also, the highly simplified diffusive dampings ν_0 and χ_0 ensure the presence of small scale dissipation to maintain regularity. For inviscid scales, linear perturbation theory gives

$$\omega = \frac{\omega_*}{2(1+k_\perp^2)}\left(1 \pm \left(1 - 4(1+k_\perp^2)\frac{v_B v_{*_p}}{v_{*_n}^2}\right)^{1/2}\right). \quad (13)$$

Note that a threshold exists (at $v_{*_n}^2/v_B v_{*_p} = 4$), that instability requires

$$k_\perp^2 > 1/4\left(\frac{v_{*_n}^2}{v_B v_{*_p}}\right) - 1$$

and that small scale modes grow faster (until the small scale dissipation cut-off is encountered). Thus, it is clearly meaningful to speak of large scale (secondary) streamer cells populated by the interaction of small scale primary modes. This is similar to avalanches in cellular automata models produced by topplings of adjacent lattice sites.

In order to study cell dynamics, it is convenient to define the low pass filtered field $\langle A\rangle_<$ by

$$\langle A\rangle_< = \int_{k_y<k_{ymin}} dk_y \int_{k_x<k_{xmin}} dk_x A_k e^{i\boldsymbol{k}\cdot\boldsymbol{x}}. \quad (14)$$

Here the bandpass effectively filters out the high $\boldsymbol{k}$ components, which hereafter are treated as background turbulence intensity, thus allowing us to focus on the large scale cell components. Note that the filter is, in general, anisotropic. The low pass filtered equations are

$$\partial_t\langle(\phi - \nabla^2\phi)\rangle_< + v_{*_n}\partial_y\langle\phi\rangle_< + v_B\partial_y\langle p\rangle_< = S_\phi \quad (15a)$$

$$\partial_t \langle p \rangle_< - v_{*_p} \partial_y \langle \phi \rangle_< = S_p \tag{15b}$$

where

$$S_\phi = -\langle \partial_x [(\partial_y \phi) \nabla^2 \phi] \rangle_< + \langle \partial_y [(\partial_x \phi) \nabla^2 \phi] \rangle_< \tag{15c}$$

$$S_p = \langle \partial_x [(\partial_y \phi) p] \rangle_< - \langle \partial_y [(\partial_x \phi) p] \rangle_< \tag{15d}$$

are the sources for the streamer cells, and represent drive by beat interaction of small scales. Observe that the self-interactions of the large scales are neglected. The alert reader may be concerned by the formal difference between the approaches used in Section 1 and here. Actually, the approaches are fundamentally similar, and only appear to be different, since the ITG mode is a reactive instability, involving two equations and often with negligible real frequency, while the drift mode is a wave destabilized by inverse dissipation. Thus, somewhat different turbulent states are modulated in these two cases. Moreover, the result of the wave kinetic derivation in Section 2 has been previously obtained, using a methodology identical to that used here, in Section 3. Hence, there is no fundamental disagreement or inconsistency between the approaches of Sections 2 and 3.

Straightforward calculation then allows us to write the sources as

$$S_\phi = \partial_x \partial_y (\langle (\partial_x \phi)^2 \rangle_< - \langle (\partial_y \phi)^2 \rangle_<) + (\partial_y^2 - \partial_x^2) \langle (\partial_x \phi)(\partial_y \phi) \rangle_< \tag{16a}$$

$$S_p = \partial_x \langle (\partial_y \phi) p \rangle_< - \partial_y \langle (\partial_x \phi) p \rangle_<. \tag{16b}$$

Here ∂_x and ∂_y acting on quantities within brackets probe only the unfiltered (large) scales. S_ϕ and S_p represent the effects of turbulent Reynolds stresses and ion thermal flux, respectively. Observe that S_ϕ is clearly quite sensitive to anisotropy of the spectrum of small scales. S_p may be further simplified by using the (broadened) quasi-linear response of p to ϕ to write

$$S_p = \partial_y \langle (\partial_x \phi) R_{\boldsymbol{k}} (\partial_y \phi) \rangle_< v_{*_p} - \partial_x \langle (\partial_y \phi) R_{\boldsymbol{k}} (\partial_y \phi) \rangle_< v_{*_p} \tag{17a}$$

where

$$R_{\boldsymbol{k}} = \Delta\omega_{\boldsymbol{k}} / (\omega_{\boldsymbol{k}}^2 + \Delta\omega_{\boldsymbol{k}}^2). \tag{17b}$$

It is interesting to examine the structure of S_ϕ and S_p in different limits. For simplicity, we will consider isotropic turbulence, so that $\langle (\partial_y \phi)^2 \rangle_< = \langle (\partial_x \phi)^2 \rangle_<$. In the 'streamer limit' $\partial_y \gg \partial_x$, so that potential and pressure perturbations of the streamer remain coupled. Note that both S_ϕ and S_p are ultimately proportional to the turbulence Reynolds stress. In the opposite, 'zonal flow limit' where $\partial_x \gg \partial_y$, $\langle \phi \rangle_<$ and $\langle p \rangle_<$ decouple, so that $\langle \phi \rangle_<$ is driven by momentum transport alone (Reynolds stress again!) while $\langle p \rangle_<$ is driven by thermal transport alone. (NB: Strictly speaking, the $\langle \phi \rangle_<$ equation must be modified in the pure zonal flow limit to reflect the fact that the electrons are not adiabatic for $k_y = k_\parallel = 0$. This change amounts to taking $1 + k_x^2 \rho^2 \to k_x^2 \rho^2$ for zonal flows.) Finally, observe that isotropic cells are not pumped unless the small scale turbulence is anisotropic.

Hereafter, we will focus on the extreme streamer cell limit, where $\partial_y \langle \phi \rangle_< \gg \partial_x \langle \phi \rangle_< \to 0$. In order to examine the stability of large scales, the modulational response of the Reynolds stress and thermal flux to streamer potential perturbations must be extracted. Thus, we write

$$\langle (\partial_x \phi)(\partial_y \phi) \rangle_< = \sum \cong \left(\frac{\delta \sum}{\delta \langle \phi \rangle_<} \right) \langle \phi \rangle_< \tag{18a}$$

$$\langle (\partial_x \phi) R_{\boldsymbol{k}} (\partial_y \phi) \rangle_< = \sum{}' \cong \left(\frac{\delta \sum'}{\delta \langle \phi \rangle_<} \right) \langle \phi \rangle_<. \tag{18b}$$

For notational convenience, from now on we write $\langle \phi \rangle_<$ as $\bar{\phi}$. Fourier analysing $\bar{\phi}$ as $\bar{\phi} = \sum_{q,\Omega} \bar{\phi}_{q,\Omega} e^{i(qy - \Omega t)}$, we then obtain the non-linear dispersion relation and eigenfrequency for streamer cells. These are:

$$\Omega^2 (1 + q^2) - \Omega (q v_{*_n}) + v_B v_{*_p} q^2 \left(1 - \frac{\delta \sum'}{\delta \bar{\phi}} \right) + i q^2 \frac{\delta \sum}{\delta \bar{\phi}} \Omega = 0 \tag{19a}$$

$$\Omega = \frac{q v_{*_n}}{2} - \frac{i q^2}{2} \frac{\delta \sum}{\delta \bar{\phi}} \pm \frac{1}{2} \left(\delta\omega^2 + \left(- 2i (q v_{*_n}) q^2 \frac{\delta \sum}{\delta \bar{\phi}} + 4 q^2 v_{*_p} v_B \frac{\delta \sum'}{\delta \bar{\phi}} \right) \right)^{1/2}. \tag{19b}$$

Eq. (19b), $\delta\omega^2 = q^2 (v_*^2 - 4 v_{*_p} v_B)$ is a measure of the deviation from marginality. We have dropped the term $(\delta \sum / \delta \bar{\phi})^2$, which is $0(e\phi/T)^4$, and have taken $1 + q^2 \cong 1$. We use adiabatic theory to determine $\delta \sum / \delta \bar{\phi}$ and $\delta \sum{}' / \delta \bar{\phi}$. For ITG turbulence, which is quite similar in its dynamics to Rayleigh–Benard convection, the adiabatic invariant is the Wigner function [15, 46]:

$$N(\boldsymbol{k}) = (1 + k^2)^2 \sum_{\boldsymbol{q}} \phi_{\boldsymbol{k}+\boldsymbol{q}} \phi_{\boldsymbol{q}-\boldsymbol{k}} e^{2i \boldsymbol{q} \cdot \boldsymbol{x}}. \tag{20}$$

Obviously here $k_x \gg k_{x,min}$ and $k_y \gg k_{y,min}$. Note that N is essentially the potential enstrophy of the underlying ITG mode vortices, which is a measure of the effective 'roton' density of the turbulence. N is conserved, up to dissipation and buoyancy drive. Thus, we can write

$$\sum = \sum_{\boldsymbol{k}>\boldsymbol{k}_{min}} \frac{k_x k_y}{(1+k^2)^2} N(\boldsymbol{k}) \tag{21a}$$

$$\sum{}' = \sum_{\boldsymbol{k}>\boldsymbol{k}_{min}} \frac{k_x k_y R_{\boldsymbol{k}}}{(1+k^2)^2} N(\boldsymbol{k}) \tag{21b}$$

so that $\delta\sum/\delta\bar{\phi}$ and $\delta\sum'/\delta\bar{\phi}$ are now easily determined using the linearized WKE. For streamer cells, the linearized WKE is

$$\frac{\partial \hat{N}}{\partial t} + v_{g,y}\frac{\partial \hat{N}}{\partial y} + \gamma_{\boldsymbol{k}}\hat{N} = \frac{\partial}{\partial y}(k_x \bar{V}_x)\frac{\partial \langle N\rangle}{\partial k_y}. \tag{22a}$$

(NB: Here $\bar{V}_x = -\partial y\bar{\phi}$, the $\boldsymbol{E}\times\boldsymbol{B}$ velocity of the streamer cell.) and the response $\hat{N}$ is thus

$$\hat{N}_{q,\Omega} = \frac{iq^2 k_x \bar{\phi}_{q,\Omega}}{\Omega - qv_{g,y} + i\gamma_{\boldsymbol{k}}}\frac{\partial\langle N\rangle}{\partial k_y}. \tag{22b}$$

It follows, then, that $\delta\sum/\delta\bar{\phi}$ is given by

$$\frac{\delta\sum}{\delta\bar{\phi}} = \sum_{\boldsymbol{k}>\boldsymbol{k}_{min}} q^2 \frac{k_x^2}{(1+k^2)^2} R(\Omega - qv_{g,y}) k_y \frac{\partial\langle N\rangle}{\partial k_y} \tag{23a}$$

$$R(\Omega - qv_{g,y}) = \gamma_{\boldsymbol{k}}/(\Omega - qv_{g,y})^2 + \gamma_{\boldsymbol{k}}^2. \tag{23b}$$

$R(\Omega - qv_{g,y})$ is the broadened resonance function for interaction between the streamer phase velocity and the ITG mode group velocity. Observe that, in contrast to the case of zero frequency zonal flows, an unambiguous quasi-linear limit of R clearly exists, i.e. as $\gamma_k \to 0$, $R \to \pi\delta(\Omega - qv_{g,y})$. $\delta\sum'/\delta\bar{\phi}$ follows similarly.

It is clear that $\delta\sum/\delta\bar{\phi} < 0$ and $\delta\sum'/\delta\bar{\phi} < 0$ for $\partial N/\partial k_y < 0$, which is virtually always the case in drift wave turbulence. Thus, streamer cells will be non-linearly excited in the absence of a population inversion. Note that drive occurs via both Reynolds stress and pressure advection coupling, and that proximity to linear marginality clearly has an important effect upon streamer evolution. To clarify this, we consider two limits. For streamers that are strongly linearly stable,

$$\Omega \cong \frac{(qv_{*_n} \pm \delta\omega)}{2} - \frac{iq^2}{2}\frac{\delta\sum}{\delta\bar{\phi}}.$$

Thus, the streamer growth rate $\gamma_q = \mathrm{Im}\,\Omega = -q^2\delta\sum/\delta\bar{\phi}$ is due to Reynolds stress coupling, and is quadratic in small scale fluctuation intensity, i.e. $\delta\sum/\delta\bar{\phi} \sim \langle N\rangle \sim (e\phi/T)^2$. Finally, using dimensional units, $\gamma_q \sim (q\rho)^4$, with $q\rho < 1$. However, for scales which are linearly marginal (so that $\delta\omega^2 = 0$),

$$\Omega = \frac{qv_{*_n}}{2} - \frac{iq^2}{2}\frac{\delta\sum}{\delta\bar{\phi}} \pm \frac{1}{2}\left(4i(qv_{*_n})q^2\frac{\delta\sum}{\delta\bar{\phi}} + 4q^2 v_{*_p}v_B\frac{\delta\sum'}{\delta\bar{\phi}}\right)^{1/2}.$$

Since $q\rho < 1$, this may be simplified to

$$\Omega \cong \frac{qv_{*_n}}{2} - \frac{iq^2}{2}\frac{\delta\sum}{\delta\bar{\phi}} \pm \left(q^2 v_{*_p}v_B\frac{\delta\sum'}{\delta\bar{\phi}}\right)^{1/2}$$

so that $\gamma_q \sim (q^2 v_{*_p}v_B)^{1/2}(e\phi/T)$. Note that near marginality, γ_q scales directly with curvature, is controlled by modulation of pressure advection and scales with $(e\phi/T)$. Thus, we can conclude that there is a regime of fast streamer drive ($\sim e\phi/T$) near marginal stability and a regime of slow drive $\sim(e\phi/T)^2$ when the large scales are stable. The crossover between these two limits occurs when $\delta\omega^2 \sim \max(iqv_{*_n}q^2\delta\sum/\delta\bar{\phi},\ q^2 v_{*_p}v_B\delta\sum'/\delta\bar{\phi})$. Note that the streamer always has a real frequency $\sim qv_{*_n}$.

While this simple study employs only local analysis, it is nevertheless possible to deduce certain aspects of streamer physics in toroidal geometry from the results obtained here. Streamers always have a finite q_y, which translates to finite n ($k_\theta = nq(r)/r$) in a torus. Except for extremely low n's, then, streamer structure should be compatible with the ballooning mode representation. Indeed, since the streamer drive $\sum \sim |\phi(\theta)|^2$ is proportional to the intensity (envelope) of the underlying ballooning–ITG modes, streamers can also be expected to extend along magnetic field lines and exhibit the other structural features of ballooning modes in a torus. Recent simulations [38] indicate that streamers indeed do exhibit such characteristics of ballooning structure, albeit with many n modes participating. This vitiates the oft stated assumption that magnetic shear, toroidicity, etc., will inhibit convective cell and streamer formation.

3.3. Self-regulation mechanisms for streamers

It is important to realize that the turbulent state with streamer cells is dynamic rather than static. In particular, while cells are pumped by small scales, they also produce feedback on the underlying ITG modes by shearing, as well as via gradient relaxation. Here it is important to note that, in contrast to

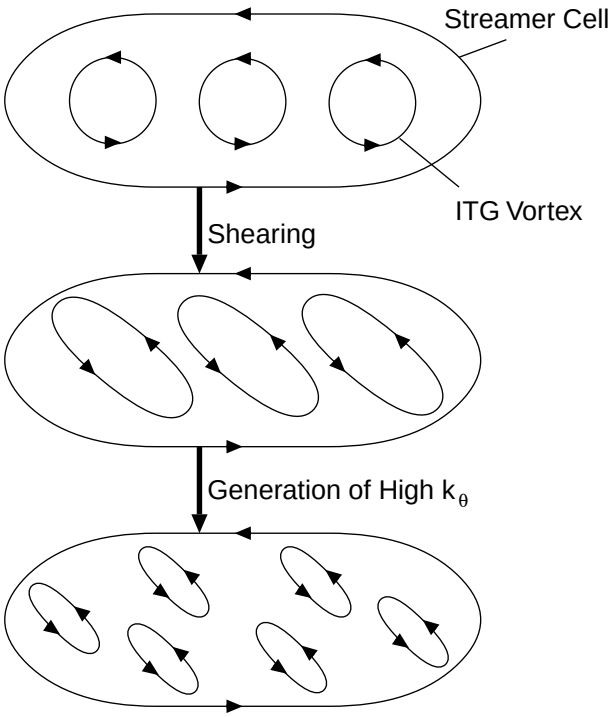

Figure 5. Poloidal shear of radial streamer flows strains and enhances the decorrelation of ITG vortices.

zonal flows, 'shearing' refers to poloidal shearing of radial streamer flows rather than the usual process of radial shearing of poloidal flows (Fig. 5). The shearing process is a stochastic one, whereby an ensemble of streamer cells induces a random walk of the ITG mode k_y, which ultimately couples ITG driven spectral energy to high k_y damping. Stochastic methodology is applicable if the underlying ITG rays are chaotic (i.e. have a positive Lyapunov exponent). In that case, standard quasi-linear theory allows us to write the WKE for $\langle N\rangle$ as:

$$\frac{\partial\langle N\rangle}{\partial t} = \frac{\partial}{\partial k_y} D_{ky} \frac{\partial\langle N\rangle}{\partial k_y} + \gamma_{\boldsymbol{k}}\langle N\rangle - \Delta\omega_{\boldsymbol{k}} \frac{\langle N\rangle^2}{N_0} \quad (24a)$$

$$D_{ky} = \sum_q q^4 k_x^2 |\bar{\phi}_q|^2 R(\Omega_q - q, v_{g,y}). \quad (24b)$$

Here D_{ky} represents the stochastic refraction of ITG eddys by poloidally sheared streamer flows [7, 8, 47]. Note, however, that in contrast to the case of its analogue for zonal flow feedback shearing, $\Omega \neq 0$ for streamers. Hence, $\langle N\rangle$ evolution can saturate by plateau formation at $\boldsymbol{k}$ such that $v_{g,y}(\boldsymbol{k}) = \Omega_q/q$. While growth and local spectral interactions can be expected to perturb the flattened $\langle N\rangle$, observation of such a plateau formation trend in simulations would be one indicator of the presence and activity of this important feedback mechanism.

Another possible feedback mechanism which may limit streamer growth is Kelvin–Helmholtz (K–H) type instability of the streamer flow [48]. In contrast to the case of zonal flows, K–H type modes for streamers are simple and robust. This is a consequence of the fact that a K–H instability is basically an interchange of two vortices across the midpoint of the shear layer. In the case of zonal flows, this interchange is a radial one, which forces the vortex tubes involved to rotate, so as to align with the local (sheared) magnetic field. Thus, K–H instabilities will be severely inhibited by magnetic shear, Landau damping, etc. For streamers, the interchange is azimuthal (at roughly constant radius) so no vortex tube rotation is required. Also, since plasma free energy is stored in radial gradients, streamer K–H modes are driven by flow shear only. Thus, well known results from hydrodynamics are applicable. In the case of long, thin streamers, which can be crudely approximated as tangential discontinuities for the case of $q_x\Delta y < 1$ (here q_x is the wavenumber of the K–H mode and $\Delta y \sim 1/q$ is the poloidal width of the streamer), the K–H growth rate will scale as $\gamma_{q_x,KH} = q_x\bar{V}/2$, where $\bar{V}$ is the streamer flow velocity.

All told, the coupled system of streamers and ITG vortices is self-regulating and clearly of the predator–prey form. It can be described by the equations

$$\frac{\partial}{\partial t}|\bar{\phi}_q|^2 = \gamma_q|\bar{\phi}_q|^2 - \gamma_{KH}|\bar{\phi}_q|^2 - \gamma_{d,q}|\bar{\phi}_q|^2 \quad (25a)$$

$$\frac{\partial\langle N\rangle}{\partial t} = \frac{\partial}{\partial k_y} D_{k_y} \frac{\partial\langle N\rangle}{\partial k_y} + \gamma_{\boldsymbol{k}}\langle N\rangle - \Delta\omega_{\boldsymbol{k}} \frac{\langle N\rangle^2}{N_0} \quad (25b)$$

together with the transport equation for mean pressure. Here γ_q is the modulation instability pumping rate, γ_{KH} is the K–H instability growth rate (both given above) and $\gamma_{d,q}$ refers to residual linear Landau and collisional damping, etc. The $\langle N\rangle$ equation is the same as Eqs (24).

It is interesting to compare the efficacy of the two non-linear self-regulation mechanisms, namely K–H instability (note $\gamma_{KH} = \gamma_{KH}(\bar{\phi})$) and random shearing. Crudely put, D_{k_y} states that random shearing will quench streamer drive at a rate $\gamma_{sh} \sim \overline{(\partial y\bar{V})^2}\tau_{ac}$, where $\overline{(\partial y\bar{V})^2}$ is the mean square poloidal shearing rate of the streamer flow field and τ_{ac} is the autocorrelation time of the streamer pattern. Estimating $\overline{(\partial y\bar{V})^2}\tau_{ac}$ as $\alpha(\partial y\bar{V})$, where α is a factor ≤ 1, it follows that $\gamma_{KH}/\gamma_{sh} \sim q_x/\alpha q_y$. Thus, it seems that

both processes will be significant and that detailed quantitative studies will be required for further elucidation of their relative strength. At this point, however, it does seem fair to say that the conventional wisdom which states that 'streamers break up via K–H instabilities' seems little more than convention.

3.4. Streamers and the statistics of transport

A quantitative theory of transport must account for and predict avalanche phenomena. As avalanches are intrinsically bursty and intermittent, such a theory must necessarily be statistical, i.e. designed to predict the pdf of the transport flux and not merely its mean value. While even approximate calculations of turbulence pdfs remain elusive [49] (though recent applications of instanton methods to very simple models such as 1-D Burgers turbulence hold promise in this regard [50, 51]), the modulational theory of streamer generation does allow us to estimate the variance of the turbulent flux. The flux variance is directly related to the streamer intensity, which can (in principle) be calculated using Eqs (25). Thus, some insight into the variance of the heat flux pdf and its dependencies can be obtained.

The ITG driven heat flux Q is given by

$$Q = -\left[\sum_{\boldsymbol{k}>\boldsymbol{k}_{min}} R_{\boldsymbol{k}} \frac{k_y^2}{(1+k^2)^2}\left(\langle N(\boldsymbol{k})\rangle + \hat{N}(\boldsymbol{k})\right)\right]\frac{\partial\langle p\rangle}{\partial r}. \tag{26}$$

Here the streamer flow induced spectral modulations $\hat{N}$ cause fluctuations $\hat{Q}$ in the heat flux about its mean value. Noting that $\hat{N}(k)$ is given by Eq. (22b), the flux perturbation $\hat{Q} = Q - \langle Q\rangle$ is

$$\hat{Q} = \sum_{\boldsymbol{k}>\boldsymbol{k}_{min}} R_{\boldsymbol{k}} \frac{k_y^2}{(1+k^2)^2}\sum_q e^{iqy} q^2 \bar{\phi}_q R(\Omega - q v_{g,y}) k_x \times \frac{\partial\langle N(k)\rangle}{\partial k_y}\left(\frac{\partial\langle p\rangle}{\partial r}\right). \tag{27}$$

Since it is not especially illuminating to display the detailed calculation of the normalized flux variance $\langle\hat{Q}^2\rangle/\langle Q\rangle^2$ here, we proceed to simply write its estimate, which can easily be shown to be

$$\frac{\langle\hat{Q}^2\rangle}{\langle Q\rangle^2} \approx \sum_q q^4|\bar{\phi}_q|^2\left(\frac{\alpha_1 k_x}{k_y v_g' \Delta k_y}\right)^2_{res}. \tag{28}$$

Here $v_g' = \partial v_{g,y}/\partial k_y$, Δk_y is the turbulence spectral width and α_1 is the power law index for $\langle N\rangle$ (i.e. $\langle N\rangle \sim (k_y)^{-\alpha_1}$. Note that since the streamer induced heat flux varies poloidally, $(\langle\hat{Q}^2\rangle/\langle Q\rangle^2)^{1/2}$ is finite while $\langle\hat{Q}\rangle/\langle Q\rangle$ vanishes. Thus, the RMS normalized heat flux perturbation $\Delta Q = (\langle\hat{Q}^2\rangle/\langle Q\rangle^2)^{1/2}$ is given by

$$\Delta Q \approx \left(\sum_q q^4|\bar{\phi}_q|^2\right)^{1/2}\left|\frac{\alpha_1 k_x}{k_y v_g' \Delta k_y}\right|_{res}. \tag{29}$$

Note that ΔQ is directly proportional to $\bar{\phi}$, the streamer fluctuation level. Not surprisingly, then, strong streamer excitation necessarily implies that the heat flux pdf has large variance. Indeed, balancing non-linear pumping growth with K–H break-up gives $\bar{v}_q \sim \gamma_q/q_x$, so

$$\Delta Q \sim (q_y\gamma_q/q_x)(\alpha_1 k_x/k_y v_g' \Delta k_y). \tag{30}$$

Several aspects of this estimate of the normalized flux variance are of interest. First, note that $\Delta Q \sim 1/q_x$, where q_x is the wavenumber of the (streamer flow) K–H instability. Thus, long wavelength K–H implies large ΔQ, since the residual cells (i.e. those produced by K–H break-up of the streamer) will be extended (i.e. $q_y \gtrsim q_x$). Note also that near marginality, $\gamma_q \sim \omega_c(e\phi/T)$ (where ω_c is the curvature frequency and $e\phi/T$ is the ITG fluctuation level). Thus, the combined influence of large γ_q and small q_x ($q_y \gtrsim q_x$) suggests that the flux variance can indeed be significant, i.e. $\Delta Q \sim 0.2$–0.5 for typical parameters. This estimate suggests that further, quantitative studies of flux statistics are most certainly warranted.

4. Conclusion

In this article, recent findings from several related investigations of secondary instability in drift wave turbulence have been presented. The principal results are:

(i) A simple physical derivation of zonal flow growth is shown to recover previously obtained theoretical results.

(ii) The coupled predator–prey type equations for the drift wave spectral intensity and the zonal flow spectrum have been solved. The solutions indicate the possibility of bifurcation transitions between states with zonal flows and 'condensate dominated' states, characterized by large eddys and increased transport. These transitions may be related to the bursting phenomena observed in gyrokinetic simulations.

(iii) Resonance broadening theory has been used to determine the effect of zonal flow shearing on the transport cross-phase. In particular, the Biglari–Diamond–Terry result [24] with $\langle v\rangle'^2 \to \langle \tilde{v}'^2\rangle$ is recovered. Since in general $\langle \tilde{v}'^2\rangle > \langle v\rangle'^2$, zonal flows have a stronger effect on the cross-phase.

(iv) The simple $K-\varepsilon$ type model of transport barrier dynamics derived previously has been extended to include the evolution of the zonal flow spectrum, as well as that of the mean flow.

(v) The rate of streamer generation has been calculated for ITG turbulence. Modulations of the vorticity flux and the thermal flux both contribute to streamer growth.

(vi) A new mechanism for streamer saturation has been identified. This mechanism is that of shearing by radial flows, which acts to increase k_θ, thus strengthening coupling to dissipation. We show that radial flow shearing is likely to be a more efficient mechanism than the oft quoted K–H instability.

(vii) The relation between the incidence of streamers and the appearance of avalanche phenomena is elucidated by the calculation of the normalized flux variance. In particular, we show that the normalized variance can approach or exceed unity when streamers are formed.

The implications of these results for various aspects of the drift wave turbulence problem are discussed.

At this point, it is reasonable to discuss possible future extensions of this work. In the area of zonal flows, the rate of zonal flow damping (i.e. 'anomalous viscosity') induced by K–H instability of zonal flows is a critical issue, as is the interplay between zonal and mean flows in transport barrier dynamics. In the area of streamers and avalanches the major challenge which remains is the non-perturbative calculation of the transport flux pdf. To this end, the application of functional integral methods from quantum field theory is a very promising approach. Finally, understanding the interplay of, and interaction between, zonal flows and streamers remains a challenging and fascinating problem.

Acknowledgements

We thank P. Beyer, S. Benkadda and X. Garbet for their collaboration on, and many useful discussions pertaining to, the subjects discussed here. We also thank C. Hidalgo, B.A. Carreras, D.E. Newman, R. Moyer, T. Rhodes and G. Tynan for stimulating conversations. This research was partially supported by US Department of Energy grant DE-FG03-88ER53275.

References

[1] Hasagewa, A., Wakatani, M., Phys. Rev. Lett. **59** (1987) 1581.
[2] Lin, Z., et al., Science **281** (1998) 1835.
[3] Beer, M., et al., Plasma Phys. Control. Fusion **35** (1993) 973.
[4] Dimits, A., et al., Phys. Rev. Lett. **77** (1996) 71.
[5] Sydora, R.D., et al., Plasma Phys. Control. Fusion **38** (1996) A281.
[6] Scott, B., Plasma Phys. Control. Fusion **34** (1992) 1977.
[7] Diamond, P.H., et al., in Fusion Energy 1998 (Proc. 17th Int. Conf. Yokohama, 1998), IAEA, Vienna (2000) CD-ROM file TH3/1, http://www.iaea.org/programmes/ripc/physics/start.htm.
[8] Champeaux, S., Diamond, P.H., Phys. Lett. A (in press).
[9] Rosenbluth, M.N., Hinton, F.L., Phys. Rev. Lett. **80** (1998) 724.
[10] Malkov, M., et al., Phys. Plasmas **8** (2001) 1553.
[11] Rogers, B., et al., Phys. Rev. Lett. **85** (2000) 5336.
[12] Chen, L., et al., Phys. Plasmas **7** (2000) 3129.
[13] Smolyakov, A., Diamond, P.H., Medvedev, M.V., Phys. Plasmas **7** (2000) 3987.
[14] Smolyakov, A., Diamond, P.H., Shevchenko, I., Phys. Plasmas **7** (2000) 1349.
[15] Smolyakov, A., Diamond, P.H., Phys. Plasmas **6** (1999) 4410.
[16] Smolyakov, A., et al., Phys. Rev. Lett. **84** (2000) 491.
[17] Kaw, P.K., Singh, R., in preparation.
[18] Das, A., et al., in preparation.
[19] Scott, B., "Electromagnetic gyrofluid turbulence in tokamak edge geometries," Theory of Fusion Plasmas, Società Italiana di Fisica, Bologna (1998) 359.
[20] Gruzinov, I., et al., in preparation.
[21] Diamond, P.H., et al., Phys. Rev. Lett. **84** (2000) 4842.
[22] Tynan, G., et al., Phys. Rev. Lett. (in press).
[23] Lin, Z., et al., Phys. Rev. Lett. **83** (1999) 3645.
[24] Biglari, H., Diamond, P.H., Terry, P.W., Phys. Fluids B **2** (1990) 1.
[25] Newman, D.E., et al., Phys. Plasmas **5** (1998) 938.
[26] Bak, P., Tang, C., Wiesenfeld, K., Phys. Rev. Lett. **59** (1987) 381.
[27] Diamond, P.H., Hahm, T.S., Phys. Plasmas **2** (1995) 3640.
[28] Politzer, P.A., Phys. Rev. Lett. **84** (2000) 1192.
[29] Carreras, B.A., et al., Phys. Rev. Lett. **83** (1999) 3653.

[30] Hidalgo, C., Asociación Euratom–CIEMAT para Fusión, personal communication, 2000.
[31] Carreras, B.A., et al., Phys. Plasmas **7** (2000) 3278.
[32] Moyer, R., paper presented at Sherwood Fusion Theory Meeting, Atlanta, 1999.
[33] Carreras, B.A., Newman, D., Lynch, V.E., Diamond, P.H., Phys. Plasmas **3** (1996) 2903.
[34] Garbet, X., Waltz, R.E., Phys. Plasmas **5** (1998) 2836.
[35] Nevins, W.M., et al., Bull. Am. Phys. Soc. **44** (1999) 260.
[36] Beyer, P., et al., Phys. Rev. Lett. **85** (2000) 4892.
[37] Drake, J.F., Guzdar, P.N., Hassam, A.B., Phys. Rev. Lett. **61** (1988) 2205.
[38] Carreras, B.A., et al., Bull. Am. Phys. Soc. **44** (1999) 197.
[39] Medvedev, M.V., Diamond, P.H., Carreras, B.A., Phys. Plasmas **3** (1996) 3745.
[40] Diamond, P.H., Hahm, T.S., Phys. Plasmas **2** (1995) 3640.
[41] Sarazin, Y., Garbet, X., Ghendrih, P., Benkadda, S., Phys. Plasmas **7** (2000) 1085.
[42] Sagdeev, R.Z., Shapiro, V.D., Shevchenko, V.I., Sov. J. Plasma Phys. **4** (1979) 306.
[43] Okuda, H., Dawson, J.M., Phys. Fluids **16** (1973) 408.
[44] Kodama, Y., Taniuti, T., J. Phys. Soc. Jpn. **47** (1979) 1706.
[45] Horton, W., Choi, D.I., Tang, W.M., Phys. Fluids **24** (1981) 1077.
[46] Dubrulle, B., Nazarenko, S., Physica D **110** (1997) 123.
[47] Balk, A., Nazarenko, S.V., Zakharov, V.E., Sov. Phys. — JETP **71** (1990) 249.
[48] Cowley, S.C., Kulsrud, R.M., Sudan, R., Phys. Fluids B **3** (1991) 2767.
[49] Pope, S.B., Annu. Rev. Fluid Mech. **26** (1994) 23.
[50] Polyakov, A.M., Phys. Rev. E **52** (1995) 6183.
[51] Gurarie, V., Migdal, A., Phys. Rev. E **54** (1996) 4908.

(Manuscript received 4 October 2000
Final manuscript accepted 22 March 2001)

E-mail address of P.H. Diamond:
pdiamond@physics.ucsd.edu

Subject classification: D2, Tt